ESA Climate Change Initiative "Plus" (CCI+)

# End-to-End ECV Uncertainty Budget (E3UB)

# -

# TROPOMI WFM-DOAS XCH$_4$

for the Essential Climate Variable (ECV)

## Greenhouse Gases (GHG)

Written by:

GHG-CCI group at IUP

Lead author: O. Schneising, IUP, Univ. Bremen, Germany

| | ESA Climate Change Initiative "Plus" (CCI+)<br><br>**End-to-End ECV Uncertainty Budget (E3UB) – TROPOMI/WFMD**<br><br>for the Essential Climate Variable (ECV) Greenhouse Gases (GHG) | |
|---|---|---|
| | | Version 7<br>(contractual version 2) |
| | | 31 May 2024 |

# Change log:

| Version Nr. | Date | Status | Reason for change |
|---|---|---|---|
| Version 1 | 23 Oct 2019 | Final | New document |
| Version 2 | 19 Dec 2019 | Final | Revision according to ESA's review |
| Version 3 | 06 Nov 2020 | Final | Update for CRDP#6 |
| Version 4 | 08 Jan 2021 | Final | Revision according to ESA's review |
| Version 5 | 09 Nov 2021 | Final | Update for CRDP#7 |
| Version 6 | 30 Mar 2023 | Final | Update for CRDP#8 |
| Version 7 | 31 May 2024 | Final | Update for CRDP#9 |

# End-to-End ECV Uncertainty Budget (E3UB)

TROPOMI WFM-DOAS (TROPOMI/WFMD) XCH$_4$

Prepared by:

Oliver Schneising

Valid for:

**TROPOMI WFM-DOAS**

| **Product** | **Version** |
|---|---|
| Methane column-averaged dry air mole fraction (XCH$_4$) | v1.8 |

# Contents

# 1 Introduction

## 1.1 Purpose of document

This E3UB provides an overview of random and systematic errors affecting the WFMD retrievals submitted for the ESA GHG-CCI+ Climate Research Data Package version 9 (CRDP#9). Application of confidence limits to the retrieval is required to translate remotely sensed data presented here into modelled estimations with a known degree of confidence, allowing detection of climate change impacts additional to the natural variability of greenhouse gases. In particular the GHG-CCI User Requirements have placed strict measurement error requirements on the participating GHG retrievals (Chevallier et al., 2014).

## 1.2 Intended Audience

This document is intended for users in the modelling community applying the WFMD products for inversions, as well as remote sensing experts interested in atmospheric soundings of XCH$_4$. In both cases the work presented here will give the user a more thorough understanding of error implicit in this GHG-CCI product.

## 1.3 Error term definition

Error terms used in this report are defined to maintain consistency with other CCI user group error terms recommended at the 2014 CCI co-location meeting. Following the descriptions of Chevallier et al. (2014) and references therein:

| | |
|---|---|
| Error | Difference between measured values and reality. |
| Systematic error | Component of measurement error that in replicate measurements remains constant or varies in a predictable manner. |
| Bias | Estimate of a systematic measurement error. |
| Precision | Reproducibility or repeatability of a measurement. Precision is a measure of the random error and can be improved by suitable averaging. |
| Stability | Systematic error over time, with random errors largely removed by averaging of observations. |
| Sensitivity | Change of measurement due to instrumental and algorithmic response to physical or simulated input parameters. |

## 2 Error sources

The majority of error is added to measurements from sources grouped into two themes - scattering of radiation into and out of the sensed light path by poorly quantified aerosol loading and cloud parameters in combination with surface reflectivity and viewing geometry; and instrumental or forward model uncertainties (e.g., calibration, spectroscopy). The aforementioned errors can be further grouped into systematic and random error components.

### 2.1 Systematic

Systematic retrieval errors include algorithmic effects such as inaccuracy in the solar and radiative transfer models, which will not change with the duration of the satellite's sensing. The same applies to restrictions in instrument calibration accuracy. Viewing geometry also affects retrievals in a regular fashion by modifying the light path of sensed radiation as a function of the position of the instrument and the sun. Interplay between increased path lengths and random error components such as aerosol optical depth add complications to the issue of measurement geometry.

### 2.2 Random

Random errors are introduced to observations at the sensing stage of a measurement by detector noise. In addition to instrument noise, atmospheric parameters are able to have effects on sounding measurements by scattering light in and out of the sensed column. Errors due to unknown aerosol parameters are particularly pronounced where the scattering and absorption effects of suspended particulate matter are poorly modelled. Scattering due to clouds which are not screened from observation record present similar problems. In addition to atmospheric parameters, specific instrument features, such as potential sensitivity nonuniformities of the detector array, also contribute to the pseudo-noise component.

## 3 Methodology

The Weighting Function Modified Differential Optical Absorption Spectroscopy (WFM-DOAS) algorithm (Buchwitz et al., 2005a,b; Schneising et al., 2008, 2009, 2011, 2012; Heymann et al., 2012a,b; Schneising et al., 2013, 2014a,b, 2019, 2020a,b, 2023) is a least-squares method based on scaling (or shifting) pre-selected atmospheric vertical profiles. The column-averaged dry air mole fractions of methane (denoted XCH$_4$) are obtained from the vertical column amounts of CH$_4$

by normalising with the air column, which is obtained from the European Centre for Medium-Range Weather Forecasts (ECMWF). The corresponding vertical column amounts of CH$_4$ are retrieved from the measured sun-normalised radiance using spectral fitting windows in the SWIR spectral region (2311-2315.5 nm and 2320-2338 nm). A post-processing machine learning-based quality filter is applied for removal of low quality retrievals (Schneising et al., 2019). An additional (post-processing) shallow learning calibration procedure is applied to minimise residual systematic retrieval biases (Schneising et al., 2019). The post-processing also includes efficient orbit-wise destriping based on combined wavelet–Fourier filtering to remove stripes in flight direction in the TROPOMI data (Schneising et al., 2023).

The error analysis is based on synthetic data and validation of the results based on real TROPOMI data with independent reference data. The validation data set is the GGG2020 collection of the Total Carbon Column Observing Network (TCCON) (Wunch et al., 2011a) (available from https://tccondata.org/). From the validation with TCCON data at the 25 TCCON sites listed in Table 3.1, realistic error estimates of the satellite data are provided.

The error analysis presented in the following is largely adopted from Schneising et al. (2019). To compare the satellite data with TCCON quantitatively, it has to be taken into account that the sensitivities of the instruments differ from each other and that individual apriori profiles are used to determine the best estimate of the true atmospheric state, respectively. The first step is to correct for the apriori contribution to the smoothing equation by adjusting the measurements for a common apriori profile (Rodgers, 2000; Dils et al., 2014; Schneising et al., 2019). Here we use the TCCON prior as the common apriori profile for all measurements:

$$\hat{c}_{\mathrm{adj}} = \hat{c} + \frac{1}{m_0} \sum_l m_l \left(1 - A_l\right) \left(x_{a,T}^l - x_a^l\right) \tag{1}$$

In this equation, $\hat{c}$ represents the originally retrieved TROPOMI column-averaged dry air mole fraction, $l$ is the index of the vertical layer, $A_l$ the corresponding column averaging kernel of the TROPOMI algorithm, $x_a$ and $x_{a,T}$ the TROPOMI and TCCON apriori dry air mole fraction profiles. $m_l$ is the mass of dry air determined from the dry air pressure difference between the upper and lower boundary of layer $l$ via $\frac{\Delta p_l}{g_l}$ with (latitude-dependent) gravitational acceleration $g_l$ and $m_0 = \sum_l m_l$ is the total mass of dry air. To minimise the smoothing error introduced by the averaging kernels we do not compare $\hat{c}_{\mathrm{adj}}$ directly with the retrieved TCCON mole fractions $\hat{c}_T$ but rather with the adjusted expression

**END-TO-END ECV UNCERTAINTY BUDGET**
TROPOMI WFM-DOAS XCH$_4$
ESA CLIMATE CHANGE INITIATIVE "PLUS" (CCI+)

INSTITUTE OF
ENVIRONMENTAL PHYSICS,
UNIVERSITY OF BREMEN

**6**

| Station | Latitude (°) | Longitude (°) | Altitude (km) | Reference GGG2020 |
|---|---|---|---|---|
| Eureka | 80.05 | −86.42 | 0.61 | Strong et al. (2022) |
| Ny-Ålesund | 78.92 | 11.92 | 0.02 | Buschmann et al. (2022) |
| Sodankylä | 67.37 | 26.63 | 0.19 | Kivi et al. (2022) |
| East Trout Lake | 54.35 | −104.99 | 0.50 | Wunch et al. (2022) |
| Bremen | 53.10 | 8.85 | 0.03 | Notholt et al. (2022) |
| Harwell | 51.57 | −1.32 | 0.14 | Weidmann et al. (2023) |
| Karlsruhe | 49.10 | 8.44 | 0.11 | Hase et al. (2022) |
| Paris | 48.85 | 2.36 | 0.06 | Té et al. (2022) |
| Orléans | 47.97 | 2.11 | 0.13 | Warneke et al. (2022) |
| Garmisch | 47.48 | 11.06 | 0.75 | Sussmann and Rettinger (2023) |
| Park Falls | 45.94 | −90.27 | 0.44 | Wennberg et al. (2022b) |
| Rikubetsu | 43.46 | 143.77 | 0.38 | Morino et al. (2022a) |
| Xianghe | 39.80 | 116.96 | 0.04 | Zhou et al. (2022) |
| Lamont | 36.60 | −97.49 | 0.32 | Wennberg et al. (2022c) |
| Tsukuba | 36.05 | 140.12 | 0.03 | Morino et al. (2022b) |
| Nicosia | 35.14 | 33.38 | 0.19 | Petri et al. (2022) |
| Edwards | 34.96 | −117.88 | 0.70 | Iraci et al. (2022) |
| Caltech | 34.14 | −118.13 | 0.24 | Wennberg et al. (2022a) |
| Saga | 33.24 | 130.29 | 0.01 | Shiomi et al. (2022) |
| Hefei | 31.90 | 119.17 | 0.04 | Liu et al. (2022) |
| Burgos | 18.53 | 120.65 | 0.04 | Morino et al. (2022c) |
| Darwin | −12.46 | 130.93 | 0.04 | Deutscher et al. (2023b) |
| Réunion | −20.90 | 55.49 | 0.09 | De Mazière et al. (2022) |
| Wollongong | −34.41 | 150.88 | 0.03 | Deutscher et al. (2023a) |
| Lauder | −45.04 | 169.68 | 0.37 | Sherlock et al. (2022) |

Table 3.1: TCCON sites used in the validation ordered according to latitude from north to south.

(Rodgers and Connor, 2003; Wunch et al., 2011b; Schneising et al., 2019)

$$\hat{c}_{T,\text{adj}} = c_{a,T} + \left( \frac{\hat{c}_T}{c_{a,T}} - 1 \right) \frac{1}{m_0} \sum_l m_l A_l x_{a,T}^l \qquad (2)$$

Thereby, $c_{a,T}$ represents the TCCON apriori column-averaged dry air mole fraction associated with the apriori profile $x_{a,T}$.

## 4 Error results

### 4.1 Error analysis based on synthetic data

#### 4.1.1 Systematic error

Several error sources were analysed using simulated measurements (Schneising et al., 2019). That means that for different scenarios defined by specific atmospheric conditions, radiances and irradiances are calculated with the radiative transfer model, which are subsequently used as measurement input in the retrieval. The errors are then defined as the deviation of the retrieved from the true quantities. The corresponding results for several scenarios are summarised in Table 4.1. All scenarios already include interpolation between different wavelength grids (for measured and reference spectra) unless otherwise stated.

The analysis includes *Basic* scenarios testing if perturbations of the state vector elements can be retrieved, quantifying look-up table interpolation errors, and analysing errors caused by off-nadir conditions. In order to examine the sensitivity to vertical profile variations, the scenario class of *Profiles* includes several realistic model atmospheres based on measurements and theoretical predictions (Anderson et al., 1986), with all methane profiles scaled to have surface values of 1850 ppb in each case to better represent current atmospheric conditions. The respective atmospheres differ from the U.S. Standard Atmosphere with respect to temperature, pressure, water vapour, carbon monoxide, and methane profiles. These scenarios are more difficult to deal with than the basic ones, because the perturbations are not consistent with the scaling assumption, i.e., they include proper variations of the profile shape.

Also examined is the sensitivity to the *Spectral albedo* of typical natural surface types. The analysed *Aerosol* scenarios are largely described in Schneising et al. (2008, 2009) with aerosol type definitions in the different atmospheric layers based on Optical Properties of Aerosols and Clouds (OPAC) (Hess et al., 1998). The retrieval errors due to undetected *Subvisual clouds* are also investigated for different ice and water clouds. Larger systematic errors occur in the case of thick clouds because clouds are not explicitly considered in the forward model of the

**END-TO-END ECV UNCERTAINTY BUDGET**
TROPOMI WFM-DOAS XCH$_4$
ESA CLIMATE CHANGE INITIATIVE "PLUS" (CCI+)

INSTITUTE OF
ENVIRONMENTAL PHYSICS,
UNIVERSITY OF BREMEN

**8**

retrieval algorithm to retain the high processing speed. However, these cases are typically filtered out reliably by the implemented quality filter.

Thus, the scenarios of Table 4.1 give an impression of the magnitude of errors one can theoretically expect after quality filtering: Typical systematic retrieval errors are below 1% for CH$_4$ even for challenging scenarios. Corresponding errors for the simultaneously retrieved CO are below 2%.

### 4.1.2 Random error

The retrieval noise is determined via error propagation from the measurement noise. To assess the theoretical precision performance, we assume a simple shot noise limited noise model, which is defined in the following way: The reference signal-to-noise ratio is $SN_{ref} = 100$ in the continuum (radiance $L_{ref} = 4.3 \cdot 10^{11}$ phot/s/cm$^2$/nm/sr) for a dark scene (albedo = 0.05) with low sun (solar zenith angle of 70°) and is scaled according to

$$SN(L) = SN_{ref} \sqrt{\frac{L}{L_{ref}}} \qquad (3)$$

for other radiances. The resulting absolute precision is widely independent of the current concentrations. For U.S. Standard atmosphere values, the corresponding relative retrieval noise for different albedos and solar zenith angles is shown in Figure 4.1. It is below 1% for solar zenith angles smaller than 75° and albedos larger than 0.03 in the case of CH$_4$. For the interested reader, the results for the simultaneously retrieved CO are also shown. As the CO absorption is considerably weaker than the CH$_4$ absorption, the CO retrieval exhibits larger relative noise, which is below 8% for albedos larger than 0.03.

**END-TO-END ECV UNCERTAINTY BUDGET**
TROPOMI WFM-DOAS XCH$_4$
ESA CLIMATE CHANGE INITIATIVE "PLUS" (CCI+)

INSTITUTE OF
ENVIRONMENTAL PHYSICS,
UNIVERSITY OF BREMEN

9

| | scenario | CH$_4$ error (%) | CO error (%) |
|---|---|---|---|
| Basic | dry run (no $\lambda$ interpol.) | 0.00 | 0.00 |
| | dry run | 0.00 | −0.03 |
| | dry run $\oplus$ | −0.08 | −0.15 |
| | dry run $\angle$ | −0.09 | −0.20 |
| | $T + 30\,\mathrm{K}$ | 0.25 | −0.24 |
| | $T - 30\,\mathrm{K}$ | 0.06 | −0.42 |
| | $p + 5\%$ | −0.01 | −0.06 |
| | $p - 5\%$ | −0.04 | −0.10 |
| | albedo 0.2 | −0.01 | −0.04 |
| Profiles | midlatitude summer | 0.12 | 0.35 |
| | midlatitude winter | −0.13 | 0.68 |
| | subarctic summer | 0.09 | 0.60 |
| | subarctic winter | 0.63 | −0.59 |
| | tropical | 0.15 | −0.94 |
| Spectral albedo | sand | −0.03 | −0.04 |
| | soil | 0.01 | −0.03 |
| | rangeland | 0.02 | −0.11 |
| | deciduous | −0.07 | 0.01 |
| | conifers | 0.01 | −0.19 |
| | snow | −0.25 | −0.30 |
| | ocean | 0.00 | −0.07 |
| Aerosols | no aerosol | 0.01 | 0.10 |
| | urban | 0.11 | 0.04 |
| | desert (sand albedo) | 0.41 | 0.40 |
| | arctic (snow albedo) | −0.19 | −0.41 |
| | extreme in boundary layer | 0.34 | −0.43 |
| | extreme in boundary layer $\oplus$ | 0.24 | −0.51 |
| | extreme in boundary layer $\angle$ | −0.28 | −1.38 |
| Subvisual clouds | cirrus | −0.29 | −0.87 |
| | cirrus $\oplus$ | −0.41 | −0.99 |
| | cirrus $\angle$ | −0.86 | −1.84 |
| | cirrus (fractal 50) | −0.33 | −0.94 |
| | cirrus (hexagonal 50×100) | 0.11 | −0.20 |
| | cirrus ($\tau$=0.05) | −0.56 | −1.53 |
| | cumulus | −0.31 | −0.86 |
| | cumulus ($R$=6 $\mu$m) | −0.21 | −0.74 |
| | cumulus ($R$=14 $\mu$m) | −0.32 | −0.87 |
| | cumulus ($\tau$=0.05) | −0.55 | −1.44 |

Table 4.1: Error analysis for different scenarios. Standard settings are direct nadir, sea level, solar zenith angle 50°, albedo 0.1, and U.S. Standard atmosphere. Scenarios with $\oplus$ include scaling of the CH$_4$ and CO profiles by 10%, for scenarios with $\angle$ the sensor zenith angle is set to 30° (relative azimuth 60°). Standard cirrus are located between 11 and 12 km (cloud optical thickness $\tau$=0.03) consisting of fractal ice crystals with an edge length of 100 $\mu$m. Standard cumulus are located between 3 and 4 km ($\tau$=0.03) consisting of water droplets with an effective radius $R$ of 10 $\mu$m.

**END-TO-END ECV UNCERTAINTY BUDGET**
TROPOMI WFM-DOAS XCH$_4$
ESA CLIMATE CHANGE INITIATIVE "PLUS" (CCI+)

INSTITUTE OF      **10**
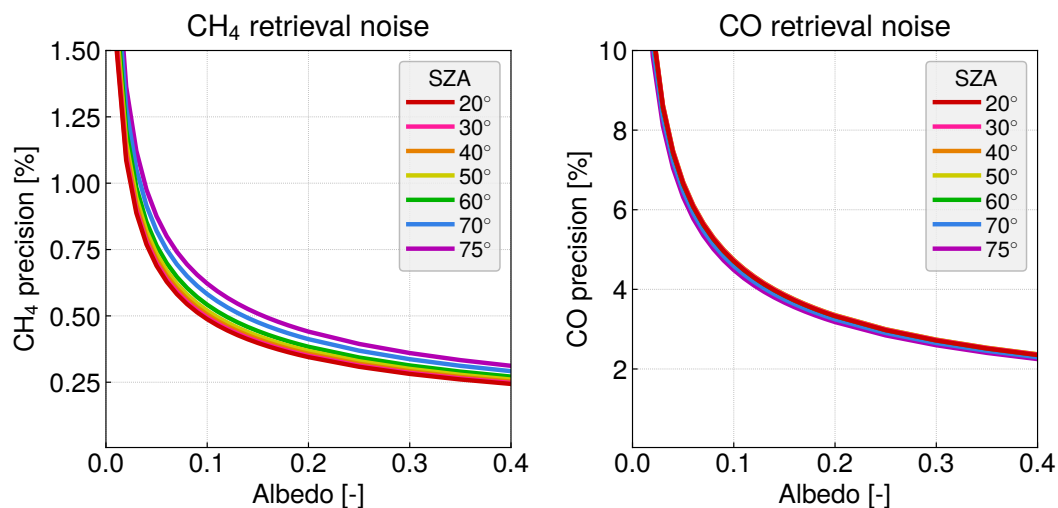ENVIRONMENTAL PHYSICS,
UNIVERSITY OF BREMEN

Figure 4.1: TROPOMI/WFM-DOAS CH$_4$ and CO relative retrieval noise for U.S. Standard atmosphere conditions.

## 4.2 Error analysis based on real data

The Climate Research Data Package version 8 (CRDP#8) WFMD data set covers the time period from November 2017 to December 2022 ensuring a comprehensive validation with Total Carbon Column Observing Network (TCCON) data (Wunch et al., 2011a).

### 4.2.1 Systematic error

The systematic error is quantified by validation with the 2020 release (GGG2020) of ground-based Fourier Transform Spectroscopy (FTS) measurements of the TCCON. To ensure comparability, all TCCON sites use similar instrumentation (Bruker IFS 125HR) and a common retrieval algorithm. The TCCON data are tied to the WMO trace gas scale using airborne in situ measurements applying individual scaling factors for each species. The estimated station-to-station accuracy ($1\sigma$) is about 3.5 ppb for XCH$_4$ (Wunch et al., 2010).

The validation results are summarised in Figure 4.2 including the mean bias $\mu$ and the scatter $\sigma$ relative to TCCON for each site. The spatial systematic error is then defined as the the standard deviation of the local offsets $\mu$ relative to TCCON at the individual sites and amounts to 5.10 ppb. The seasonal systematic error is defined as the standard deviation of the four overall seasonal offsets (using all sites combined after subtraction of the respective local offsets) relative to TCCON and amounts to 1.19 ppb. The spatio-temporal systematic error (defined as the
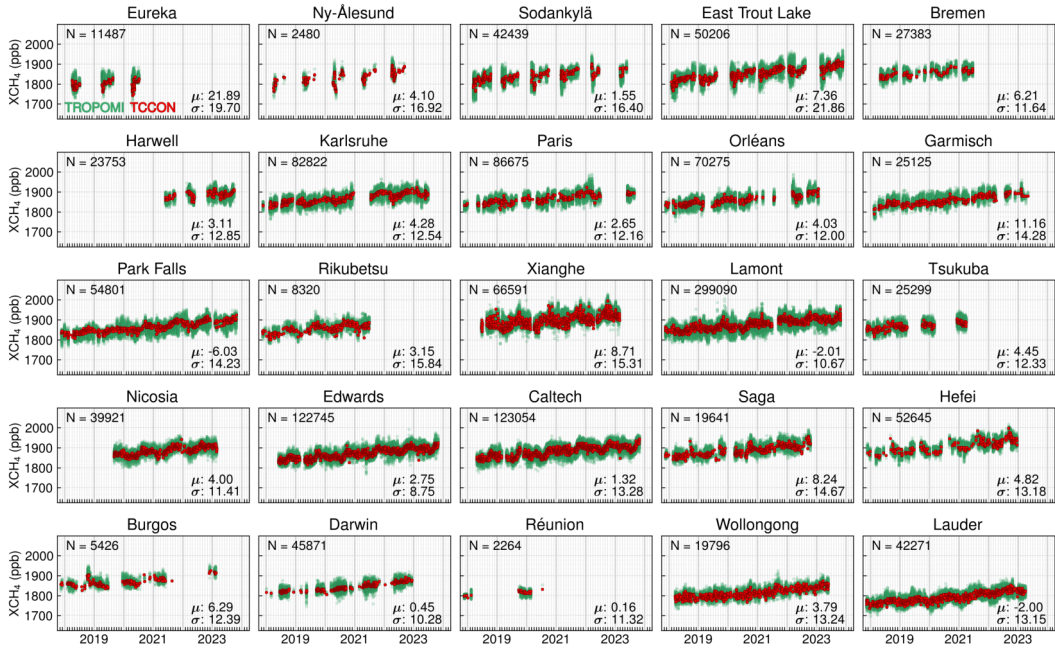
**END-TO-END ECV UNCERTAINTY BUDGET**
TROPOMI WFM-DOAS XCH₄
ESA CLIMATE CHANGE INITIATIVE "PLUS" (CCI+)

INSTITUTE OF
ENVIRONMENTAL PHYSICS,
UNIVERSITY OF BREMEN

**11**

Figure 4.2: Comparison of the TROPOMI/WFMD v1.8 XCH₄ time series (green) with ground based measurements from the TCCON (red). For each site, $N$ is the number of collocations, $\mu$ corresponds to the mean bias and $\sigma$ to the scatter of the satellite data relative to TCCON in ppb.

the root-sum-square of the spatial and seasonal systematic errors) amounts to 5.24 ppb, which is on the order of the estimated (station-to-station) accuracy of the TCCON of about 3.5 ppb. The local offsets have considerably changed at some sites between GGG2014 and GGG2020, e.g. there is an increased offset at Eureka, without resulting in an obvious improvement in agreement with TROPOMI/WFMD.

### 4.2.2 Global offset

The global offset relative to the validation data is defined as the mean of the local biases at the individual sites and amounts to 4.18 ppb when using GGG2020 (was 0.80 ppb for GGG2014 and CRDP#8). Thereby, the absolute level of the satellite data is independent of TCCON, it was neither adapted to one nor to the other GGG version.
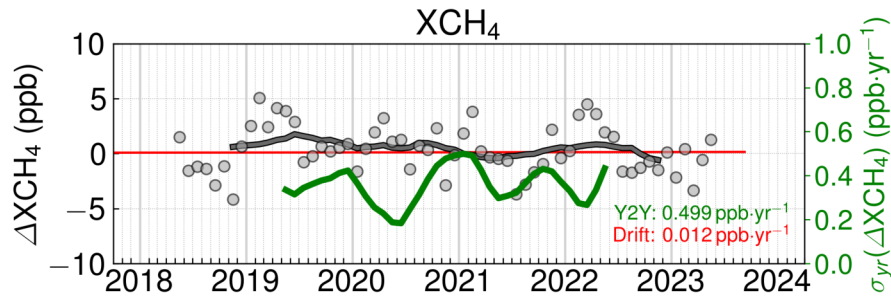
Figure 4.3: Long-term drift and year-to-year stability at TCCON sites.

### 4.2.3 Stability

To analyse the stability, we use comparisons with the TCCON since the start of the routine operations phase of Sentinel-5P to have sufficient data coverage. To assess the long-term drift stability, a robust regression (Huber and Ronchetti, 2009) of the monthly mean differences relative to the reference (using all data combined after subtraction of the respective regional offsets) with time is used. The resulting stability estimate is $0.01 \, \text{ppb·yr}^{-1}$ (see red straight line in Figure 4.3).

The year-to-year stability allowing to detect potential jumps in the time series is defined in the following way: The one-year moving average of the differences relative to the reference (grey curve in Figure 4.3) is generated. For a given point in time $t$, let $\sigma_{yr}(t)$ be defined as the standard deviation of this deseasonalised difference within a one-year window around $t$ (green curve in Figure 4.3). The year-to-year stability is then defined as the maximum of $\sigma_{yr}(t)$ over time, which amounts to $0.50 \, \text{ppb·yr}^{-1}$ here. Due to the moving average and the one-year moving standard deviation procedure, the green curve loses one year of data at the beginning and end of the time series.

### 4.2.4 Random error

The random error is estimated from the global scatter of the differences to TCCON after subtraction of the respective regional biases and amounts to 12.35 ppb. The corresponding scatter per site $\sigma$ is shown in Figure 4.2.

### 4.2.5 Correlations

To assess the sensitivity of the retrieval results to several parameters, it is analysed to what extent the difference to TCCON is correlated with these parameters. The square of the correlation coefficient $r^2$ is a measure of how much of the difference to TCCON can potentially be explained by sensitivity to the respective parameter.

As can be seen in Table 4.2, there are no indications for significant biases caused by the analysed parameters.

| Parameter | $r^2$ (%) |
|---|---|
| Sensor zenith angle | 0.348 |
| Albedo (2313 nm) | 0.194 |
| Cloud parameter $r_{cld}$ | 0.190 |
| H$_2$O column | 0.071 |
| Altitude | 0.034 |
| Solar zenith angle | 0.027 |

Table 4.2: Sensitivity analysis of TROPOMI/WFMD v1.8 XCH$_4$ to several parameters by analysing the correlation of the difference to TCCON with these parameters.

### 4.2.6 Reported uncertainty

The uncertainty of TROPOMI/WFMD v1.8 XCH$_4$ is estimated during the inversion procedure via error propagation from the uncorrelated spectral measurement errors $\sigma_i$ given in the TROPOMI Level 1 files. The (unknown) pseudo-noise component determined by specific atmospheric parameters or instrumental features is not considered and thus the estimated uncertainty is typically underestimating the actual uncertainty. Therefore, the reported uncertainties include a correction based on a comparison to the measured scatter relative to the TCCON to obtain a more realistic uncertainty estimate:

$$\hat{\sigma} = \frac{4}{3} \cdot (\sigma + 5\,\text{ppb}) \qquad (4)$$

After dividing up the reported uncertainties in equal sized bins of about 20000 measurements each, a robust regression (Huber and Ronchetti, 2009) provides the results shown in Figure 4.4 (neglecting the random and systematic errors of the TCCON measurements) confirming that the reported estimates are realistic.
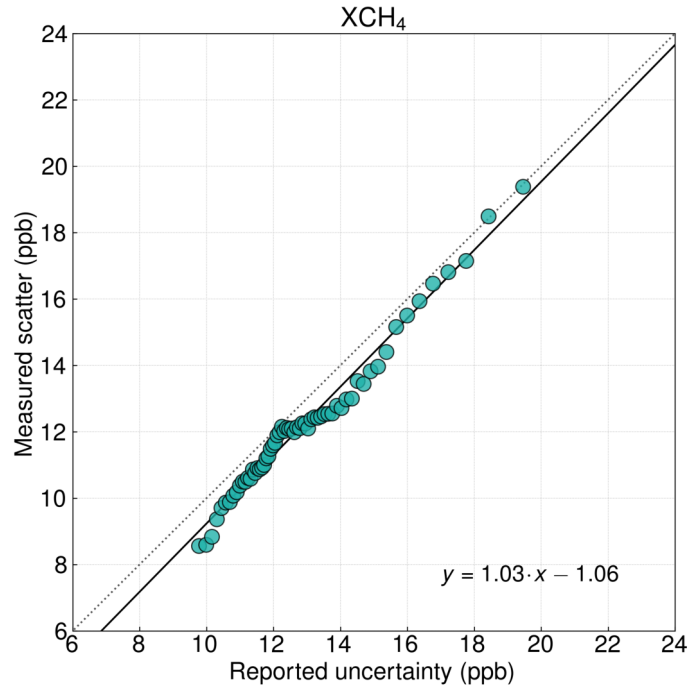
**END-TO-END ECV UNCERTAINTY BUDGET**
TROPOMI WFM-DOAS XCH$_4$
ESA CLIMATE CHANGE INITIATIVE "PLUS" (CCI+)

INSTITUTE OF
ENVIRONMENTAL PHYSICS,
UNIVERSITY OF BREMEN

**14**



Figure 4.4: Comparison of the reported uncertainty of TROPOMI/WFMD v1.8 XCH$_4$ with the measured scatter relative to the TCCON after dividing up the reported uncertainties in equal sized bins.

## 5 Summary

An analysis based on simulated measurements suggests that typical systematic retrieval errors after quality filtering are below 1%. The validation with TCCON provides realistic error estimates. The corresponding error characteristics are summarised in Table 5.1. A correlation analysis confirms that there are no indications for significant biases caused by the analysed parameters.

The reported uncertainties include a correction because the original uncertainties determined during the inversion procedure are too optimistic as they only comprise the propagated measurement errors given in the Level 1 files. Based on a comparison to the TCCON, it is concluded that the uncertainties finally reported in the product files are realistic.

| Sensor | Algorithm | Random error (ppb) | Systematic error (spatio-temporal) (ppb) | Global offset (ppb) | Stability (ppb·yr$^{-1}$) |
|--------|-----------|--------------------|------------------------------------------|---------------------|---------------------------|
| TROPOMI | WFMD v1.8 | 12.35 | 5.24 | 4.18 | Long-term Drift: 0.01<br>Year-to-year: 0.50 |

Table 5.1: TROPOMI/WFMD v1.8 XCH$_4$ error characteristics. The figures of merit are derived for the TCCON release GGG2020. The corresponding numbers for GGG2014 with different spatial and temporal coverage are given in brackets.

# References

Anderson, G. P., Clough, S. A., Kneizys, F. X., Chetwynd, J. H., and Shettle, E. P.: AFGL Atmospheric Constituent Profiles (0-120 km), Environmental Research Papers, NO. 954, AFGL-TR-86-0110, URL https://apps.dtic.mil/dtic/tr/fulltext/u2/a175173.pdf, 1986.

Buchwitz, M., de Beek, R., Burrows, J. P., Bovensmann, H., Warneke, T., Notholt, J., Meirink, J. F., Goede, A. P. H., Bergamaschi, P., Körner, S., Heimann, M., and Schulz, A.: Atmospheric methane and carbon dioxide from SCIAMACHY satellite data: initial comparison with chemistry and transport models, Atmos. Chem. Phys., 5, 941–962, https://doi.org/10.5194/acp-5-941-2005, 2005a.

Buchwitz, M., de Beek, R., Noël, S., Burrows, J. P., Bovensmann, H., Bremer, H., Bergamaschi, P., Körner, S., and Heimann, M.: Carbon monoxide, methane and carbon dioxide columns retrieved from SCIAMACHY by WFM-DOAS: year 2003 initial data set, Atmos. Chem. Phys., 5, 3313–3329, https://doi.org/10.5194/acp-5-3313-2005, 2005b.

Buschmann, M., Petri, C., Palm, M., Warneke, T., and Notholt, J.: TCCON data from Ny-Ålesund, Svalbard (NO), Release GGG2020.R0. TCCON data archive, hosted by CaltechDATA, California Institute of Technology, https://doi.org/10.14291/tccon.ggg2020.nyalesund01.R0, 2022.

Chevallier, C., Bergamaschi, P., Houweling, S., van Leeuwen, T., and Palmer, P. I.: User Requirements Document (URD) for the GHG-CCI project of ESA's Climate Change Initiative, version 2, 2014.

**END-TO-END ECV UNCERTAINTY BUDGET**
TROPOMI WFM-DOAS XCH$_4$
ESA CLIMATE CHANGE INITIATIVE "PLUS" (CCI+)

INSTITUTE OF
ENVIRONMENTAL PHYSICS,
UNIVERSITY OF BREMEN

**16**

De Mazière, M., Sha, M. K., Desmet, F., Hermans, C., Scolas, F., Kumps, N., Zhou, M., Metzger, J.-M., Duflot, V., and Cammas, J.-P.: TCCON data from Réunion Island (RE), Release GGG2020.R0. TCCON data archive, hosted by CaltechDATA, California Institute of Technology, https://doi.org/10.14291/tccon.ggg2020.reunion01.R0, 2022.

Deutscher, N. M., Griffith, D. W., Paton-Walsh, C., Jones, N. B., Velazco, V. A., Wilson, S. R., Macatangay, R. C., Kettlewell, G. C., Buchholz, R. R., Riggenbach, M. O., Bukosa, B., John, S. S., Walker, B. T., and Nawaz, H.: TCCON data from Wollongong (AU), Release GGG2020.R0. TCCON data archive, hosted by CaltechDATA, California Institute of Technology, https://doi.org/10.14291/tccon.ggg2020.wollongong01.R0, 2023a.

Deutscher, N. M., Griffith, D. W., Paton-Walsh, C., Velazco, V. A., Wennberg, P. O., Blavier, J.-F., Washenfelder, R. A., Yavin, Y., Keppel-Aleks, G., Toon, G. C., Jones, N. B., Kettlewell, G. C., Connor, B. J., Macatangay, R. C., Wunch, D., Roehl, C., and Bryant, G. W.: TCCON data from Darwin (AU), Release GGG2020.R0. TCCON data archive, hosted by CaltechDATA, California Institute of Technology, https://doi.org/10.14291/tccon.ggg2020.darwin01.R0, 2023b.

Dils, B., Buchwitz, M., Reuter, M., Schneising, O., Boesch, H., Parker, R., Guerlet, S., Aben, I., Blumenstock, T., Burrows, J. P., Butz, A., Deutscher, N. M., Frankenberg, C., Hase, F., Hasekamp, O. P., Heymann, J., De Mazière, M., Notholt, J., Sussmann, R., Warneke, T., Griffith, D., Sherlock, V., and Wunch, D.: The Greenhouse Gas Climate Change Initiative (GHG-CCI): comparative validation of GHG-CCI SCIAMACHY/ENVISAT and TANSO-FTS/GOSAT CO$_2$ and CH$_4$ retrieval algorithm products with measurements from the TCCON, Atmos. Meas. Tech., 7, 1723–1744, https://doi.org/10.5194/amt-7-1723-2014, 2014.

Hase, F., Herkommer, B., Groß, J., Blumenstock, T., Kiel, M., and Dohe, S.: TCCON data from Karlsruhe (DE), Release GGG2020.R0. TCCON data archive, hosted by CaltechDATA, California Institute of Technology, https://doi.org/10.14291/tccon.ggg2020.karlsruhe01.R0, 2022.

Hess, M., Koepke, P., and Schult, I.: Optical Properties of Aerosols and Clouds: The Software Package OPAC, Bull. Am. Met. Soc., 79, 831–844, 1998.

Heymann, J., Schneising, O., Reuter, M., Buchwitz, M., Rozanov, V. V., Velazco, V. A., Bovensmann, H., and Burrows, J. P.: SCIAMACHY WFM-DOAS XCO$_2$:

**END-TO-END ECV UNCERTAINTY BUDGET**
TROPOMI WFM-DOAS XCH$_4$
ESA CLIMATE CHANGE INITIATIVE "PLUS" (CCI+)

INSTITUTE OF
ENVIRONMENTAL PHYSICS,
UNIVERSITY OF BREMEN

**17**

comparison with CarbonTracker XCO$_2$ focusing on aerosols and thin clouds, Atmos. Meas. Tech., 5, 1935–1952, https://doi.org/10.5194/amt-5-1935-2012, 2012a.

Heymann, J., Bovensmann, H., Buchwitz, M., Burrows, J. P., Deutscher, N. M., Notholt, J., Rettinger, M., Reuter, M., Schneising, O., Sussmann, R., and Warneke, T.: SCIAMACHY WFM-DOAS XCO$_2$: reduction of scattering related errors, Atmos. Meas. Tech., 5, 2375–2390, https://doi.org/10.5194/amt-5-2375-2012, 2012b.

Huber, P. J. and Ronchetti, E. M.: Robust statistics, Wiley, New York, 2009.

Iraci, L. T., Podolske, J. R., Roehl, C., Wennberg, P. O., Blavier, J.-F., Allen, N., Wunch, D., and Osterman, G. B.: TCCON data from Edwards (US), Release GGG2020.R0. TCCON data archive, hosted by CaltechDATA, California Institute of Technology, https://doi.org/10.14291/tccon.ggg2020.edwards01.R0, 2022.

Kivi, R., Heikkinen, P., and Kyrö, E.: TCCON data from Sodankylä (FI), Release GGG2020.R0. TCCON data archive, hosted by CaltechDATA, California Institute of Technology, https://doi.org/10.14291/tccon.ggg2020.sodankyla01.R0, 2022.

Liu, C., Wang, W., Sun, Y., and Shan, C.: TCCON data from Hefei (PRC), Release GGG2020.R0, https://doi.org/10.14291/tccon.ggg2020.hefei01.R0. TCCONdataarchive,hostedbyCaltechDATA,CaliforniaInstituteofTechnology, 2022.

Morino, I., Ohyama, H., Hori, A., and Ikegami, H.: TCCON data from Rikubetsu (JP), Release GGG2020.R0. TCCON data archive, hosted by CaltechDATA, California Institute of Technology, https://doi.org/10.14291/tccon.ggg2020.rikubetsu01.R0, 2022a.

Morino, I., Ohyama, H., Hori, A., and Ikegami, H.: TCCON data from Tsukuba (JP), 125HR, Release GGG2020.R0. TCCON data archive, hosted by CaltechDATA, California Institute of Technology, https://doi.org/10.14291/tccon.ggg2020.tsukuba02.R0, 2022b.

Morino, I., Velazco, V. A., Hori, A., Uchino, O., and Griffith, D. W. T.: TCCON data from Burgos, Ilocos Norte (PH), Release GGG2020.R0. TCCON data archive, hosted by CaltechDATA, California Institute of Technology, https://doi.org/10.14291/tccon.ggg2020.burgos01.R0, 2022c.

**END-TO-END ECV UNCERTAINTY BUDGET**
TROPOMI WFM-DOAS XCH$_4$
ESA CLIMATE CHANGE INITIATIVE "PLUS" (CCI+)

INSTITUTE OF
ENVIRONMENTAL PHYSICS,
UNIVERSITY OF BREMEN

**18**

Notholt, J., Petri, C., Warneke, T., and Buschmann, M.: TCCON data from Bremen (DE), Release GGG2020.R0. TCCON data archive, hosted by CaltechDATA, California Institute of Technology, https://doi.org/10.14291/tccon.ggg2020.bremen01.R0, 2022.

Petri, C., Vrekoussis, M., Rousogenous, C., Warneke, T., Sciare, J., and Notholt, J.: TCCON data from Nicosia (CY), Release GGG2020.R0. TCCON data archive, hosted by CaltechDATA, California Institute of Technology, https://doi.org/10.14291/tccon.ggg2020.nicosia01.R0, 2022.

Rodgers, C. D.: Inverse Methods for Atmospheric Sounding: Theory and Practice, World Scientific Publishing, 2000.

Rodgers, C. D. and Connor, B. J.: Intercomparison of remote sounding instruments, J. Geophys. Res., 108, https://doi.org/10.1029/2002JD002299, 2003.

Schneising, O., Buchwitz, M., Burrows, J. P., Bovensmann, H., Reuter, M., Notholt, J., Macatangay, R., and Warneke, T.: Three years of greenhouse gas column-averaged dry air mole fractions retrieved from satellite - Part 1: Carbon dioxide, Atmos. Chem. Phys., 8, 3827–3853, https://doi.org/10.5194/acp-8-3827-2008, 2008.

Schneising, O., Buchwitz, M., Burrows, J. P., Bovensmann, H., Bergamaschi, P., and Peters, W.: Three years of greenhouse gas column-averaged dry air mole fractions retrieved from satellite - Part 2: Methane, Atmos. Chem. Phys., 9, 443–465, https://doi.org/10.5194/acp-9-443-2009, 2009.

Schneising, O., Buchwitz, M., Reuter, M., Heymann, J., Bovensmann, H., and Burrows, J. P.: Long-term analysis of carbon dioxide and methane column-averaged mole fractions retrieved from SCIAMACHY, Atmos. Chem. Phys., 11, 2863–2880, https://doi.org/10.5194/acp-11-2863-2011, 2011.

Schneising, O., Bergamaschi, P., Bovensmann, H., Buchwitz, M., Burrows, J. P., Deutscher, N. M., Griffith, D. W. T., Heymann, J., Macatangay, R., Messerschmidt, J., Notholt, J., Rettinger, M., Reuter, M., Sussmann, R., Toon, G. C., Velazco, V. A., Warneke, T., Wennberg, P. O., and Wunch, D.: Atmospheric greenhouse gases retrieved from SCIAMACHY: Comparison to ground-based FTS measurements and model results, Atmos. Chem. Phys., 12, 1527–1540, https://doi.org/10.5194/acp-12-1527-2012, 2012.

Schneising, O., Heymann, J., Buchwitz, M., Reuter, M., Bovensmann, H., and Burrows, J. P.: Anthropogenic carbon dioxide source areas observed from space:

**END-TO-END ECV UNCERTAINTY BUDGET**
TROPOMI WFM-DOAS XCH$_4$
ESA CLIMATE CHANGE INITIATIVE "PLUS" (CCI+)

INSTITUTE OF
ENVIRONMENTAL PHYSICS,
UNIVERSITY OF BREMEN

**19**

assessment of regional enhancements and trends, Atmos. Chem. Phys., 13, 2445–2454, https://doi.org/10.5194/acp-13-2445-2013, 2013.

Schneising, O., Reuter, M., Buchwitz, M., Heymann, J., Bovensmann, H., and Burrows, J. P.: Terrestrial carbon sink observed from space: variation of growth rates and seasonal cycle amplitudes in response to interannual surface temperature variability, Atmos. Chem. Phys., 14, 133–141, https://doi.org/10.5194/acp-14-133-2014, 2014a.

Schneising, O., Burrows, J. P., Dickerson, R. R., Buchwitz, M., Reuter, M., and Bovensmann, H.: Remote sensing of fugitive methane emissions from oil and gas production in North American tight geologic formations, Earth's Future, 2, 548–558, https://doi.org/10.1002/2014EF000265, 2014b.

Schneising, O., Buchwitz, M., Reuter, M., Bovensmann, H., Burrows, J. P., Borsdorff, T., Deutscher, N. M., Feist, D. G., Griffith, D. W. T., Hase, F., Hermans, C., Iraci, L. T., Kivi, R., Landgraf, J., Morino, I., Notholt, J., Petri, C., Pollard, D. F., Roche, S., Shiomi, K., Strong, K., Sussmann, R., Velazco, V. A., Warneke, T., and Wunch, D.: A scientific algorithm to simultaneously retrieve carbon monoxide and methane from TROPOMI onboard Sentinel-5 Precursor, Atmos. Meas. Tech., 12, 6771–6802, https://doi.org/10.5194/amt-12-6771-2019, 2019.

Schneising, O., Buchwitz, M., Reuter, M., Bovensmann, H., and Burrows, J. P.: Severe Californian wildfires in November 2018 observed from space: the carbon monoxide perspective, Atmos. Chem. Phys., 20, 3317–3332, https://doi.org/10.5194/acp-20-3317-2020, 2020a.

Schneising, O., Buchwitz, M., Reuter, M., Vanselow, S., Bovensmann, H., and Burrows, J. P.: Remote sensing of methane leakage from natural gas and petroleum systems revisited, Atmos. Chem. Phys., 20, 9169–9182, https://doi.org/10.5194/acp-20-9169-2020, 2020b.

Schneising, O., Buchwitz, M., Hachmeister, J., Vanselow, S., Reuter, M., Buschmann, M., Bovensmann, H., and Burrows, J. P.: Advances in retrieving XCH$_4$ and XCO from Sentinel-5 Precursor: improvements in the scientific TROPOMI/WFMD algorithm, Atmos. Meas. Tech., 16, 669–694, https://doi.org/10.5194/amt-16-669-2023, 2023.

Sherlock, V., Connor, B., Robinson, J., Shiona, H., Smale, D., and Pollard, D. F.: TCCON data from Lauder (NZ), 125HR, Release GGG2020.R0. TCCON data archive, hosted by CaltechDATA, California Institute of Technology, https://doi.org/10.14291/tccon.ggg2020.lauder02.R0, 2022.

**END-TO-END ECV UNCERTAINTY BUDGET**
TROPOMI WFM-DOAS XCH$_4$
ESA CLIMATE CHANGE INITIATIVE "PLUS" (CCI+)

INSTITUTE OF
ENVIRONMENTAL PHYSICS,
UNIVERSITY OF BREMEN

20

Shiomi, K., Kawakami, S., Ohyama, H., Arai, K., Okumura, H., Ikegami, H., and Usami, M.: TCCON data from Saga (JP), Release GGG2020.R0. TCCON data archive, hosted by CaltechDATA, California Institute of Technology, https://doi.org/10.14291/tccon.ggg2020.saga01.R0, 2022.

Strong, K., Roche, S., Franklin, J. E., Mendonca, J., Lutsch, E., Weaver, D., Fogal, P. F., Drummond, J. R., Batchelor, R., Lindenmaier, R., and McGee, E.: TCCON data from Eureka (CA), Release GGG2020.R0. TCCON data archive, hosted by CaltechDATA, California Institute of Technology, https://doi.org/10.14291/tccon.ggg2020.eureka01.R0, 2022.

Sussmann, R. and Rettinger, M.: TCCON data from Garmisch (DE), Release GGG2020.R0. TCCON data archive, hosted by CaltechDATA, California Institute of Technology, https://doi.org/10.14291/tccon.ggg2020.garmisch01.R0, 2023.

Té, Y., Jeseck, P., and Janssen, C.: TCCON data from Paris (FR), Release GGG2020.R0. TCCON data archive, hosted by CaltechDATA, California Institute of Technology, https://doi.org/10.14291/tccon.ggg2020.paris01.R0, 2022.

Warneke, T., Petri, C., Notholt, J., and Buschmann, M.: TCCON data from Orléans (FR), Release GGG2020.R0. TCCON data archive, hosted by CaltechDATA, California Institute of Technology, https://doi.org/10.14291/tccon.ggg2020.orleans01.R0, 2022.

Weidmann, D., Brownsword, R., and Doniki, S.: TCCON data from Harwell (UK), Release GGG2020.R0. TCCON data archive, hosted by CaltechDATA, California Institute of Technology, https://doi.org/10.14291/tccon.ggg2020.harwell01.R0, 2023.

Wennberg, P. O., Roehl, C., Wunch, D., Blavier, J.-F., Toon, G. C., Allen, N. T., Treffers, R., and Laughner, J.: TCCON data from Caltech (US), Release GGG2020.R0. TCCON data archive, hosted by CaltechDATA, California Institute of Technology, https://doi.org/10.14291/tccon.ggg2020.pasadena01.R0, 2022a.

Wennberg, P. O., Roehl, C. M., Wunch, D., Toon, G. C., Blavier, J.-F., Washenfelder, R., Keppel-Aleks, G., and Allen, N. T.: TCCON data from Park Falls (US), Release GGG2020.R1. TCCON data archive, hosted by CaltechDATA, California Institute of Technology, https://doi.org/10.14291/tccon.ggg2020.parkfalls01.R1, 2022b.

**END-TO-END ECV UNCERTAINTY BUDGET**
TROPOMI WFM-DOAS XCH$_4$
ESA CLIMATE CHANGE INITIATIVE "PLUS" (CCI+)

INSTITUTE OF
ENVIRONMENTAL PHYSICS,
UNIVERSITY OF BREMEN

**21**

Wennberg, P. O., Wunch, D., Roehl, C. M., Blavier, J.-F., Toon, G. C., and Allen, N. T.: TCCON data from Lamont (US), Release GGG2020.R0. TCCON data archive, hosted by CaltechDATA, California Institute of Technology, https://doi.org/10.14291/tccon.ggg2020.lamont01.R0, 2022c.

Wunch, D., Toon, G. C., Wennberg, P. O., Wofsy, S. C., Stephens, B. B., Fischer, M. L., Uchino, O., Abshire, J. B., Bernath, P., Biraud, S. C., Blavier, J.-F. L., Boone, C., Bowman, K. P., Browell, E. V., Campos, T., Connor, B. J., Daube, B. C., Deutscher, N. M., Diao, M., Elkins, J. W., Gerbig, C., Gottlieb, E., Griffith, D. W. T., Hurst, D. F., Jiménez, R., Keppel-Aleks, G., Kort, E. A., Macatangay, R., Machida, T., Matsueda, H., Moore, F., Morino, I., Park, S., Robinson, J., Roehl, C. M., Sawa, Y., Sherlock, V., Sweeney, C., Tanaka, T., and Zondlo, M. A.: Calibration of the Total Carbon Column Observing Network using aircraft profile data, Atmos. Meas. Tech., 3, 1351–1362, https://doi.org/10.5194/amt-3-1351-2010, 2010.

Wunch, D., Toon, G. C., Blavier, J.-F. L., Washenfelder, R. A., Notholt, J., Connor, B. J., Griffith, D. W. T., Sherlock, V., and Wennberg, P. O.: The Total Carbon Column Observing Network, Phil. Trans. R. Soc. A, 369, 2087–2112, https://doi.org/10.1098/rsta.2010.0240, 2011a.

Wunch, D., Wennberg, P. O., Toon, G. C., Connor, B. J., Fisher, B., Osterman, G. B., Frankenberg, C., Mandrake, L., O'Dell, C., Ahonen, P., Biraud, S. C., Castano, R., Cressie, N., Crisp, D., Deutscher, N. M., Eldering, A., Fisher, M. L., Griffith, D. W. T., Gunson, M., Heikkinen, P., Keppel-Aleks, G., Kyrö, E., Lindenmaier, R., Macatangay, R., Mendonca, J., Messerschmidt, J., Miller, C. E., Morino, I., Notholt, J., Oyafuso, F. A., Rettinger, M., Robinson, J., Roehl, C. M., Salawitch, R. J., Sherlock, V., Strong, K., Sussmann, R., Tanaka, T., Thompson, D. R., Uchino, O., Warneke, T., and Wofsy, S. C.: A method for evaluating bias in global measurements of CO$_2$ total columns from space, Atmos. Chem. Phys., 11, 12 317–12 337, https://doi.org/10.5194/acp-11-12317-2011, 2011b.

Wunch, D., Mendonca, J., Colebatch, O., Allen, N. T., Blavier, J.-F., Kunz, K., Roche, S., Hedelius, J., Neufeld, G., Springett, S., Worthy, D., Kessler, R., and Strong, K.: TCCON data from East Trout Lake, SK (CA), Release GGG2020.R0. TCCON data archive, hosted by CaltechDATA, California Institute of Technology, https://doi.org/10.14291/tccon.ggg2020.easttroutlake01.R0, 2022.

Zhou, M., Wang, P., Kumps, N., Hermans, C., and Nan, W.: TCCON data from Xianghe, China, Release GGG2020.R0. TCCON data archive, hosted by CaltechDATA, California Institute of Technology, https://doi.org/10.14291/tccon.ggg2020.xianghe01.R0, 2022.